CYBERNETICS AND PHYSICS, VOL. 14, NO. 4, 2025, 392–397

VIBRATION MECHATRONIC SETUP WITH TECHNOLOGIC EQUIPMENT: MODELING AND REDUCED ENERGY CONTROL

Oleg Shagniev
Control of Complex Systems Lab
Institute of Problems of Mechanical Engineering of RAS
Advanced Engineering School "Digital Engineering"
Peter the Great St.Petersburg Polytechnic University
Russia
shagnoleg@yandex.ru

Article history:
Received 09.12.2025, Accepted 20.12.2025

Abstract

Improving the performance of technological operations is an urgent task of modern science. Vibrational equipment is one of the common types of industrial equipment used for operations such as sieving, crushing, vibration conveying, etc. An energy-based approach to controlling vibration units allows maintaining a constant level of the total oscillation energy of the vibration unit with a load, which opens up wide opportunities for intellectualizing equipment control under conditions of parameter space uncertainty. This work aims to study the influence of the completeness of information about the vibrational state of the system on the performance of the speed gradient algorithm when controlling multiple synchronization of rotors of a vibration unit. The paper presents results of numerical simulation based on the system dynamics equations and approximate values of the vibration unit parameters. Results of experimental studies on the mechatronic vibration setup SV-2M are presented.

Key words

Vibration setup, speed gradient algorithm, control system, multiple synchronization.

1 Introduction

Vibrational equipment is used in various technological processes, including sieving of bulk media, vibration conveying, etc. The desire to improve the performance of technological operations necessitates the development of control systems that ensure high-quality synchronization of vibration setup rotors over a wide range of parameters [Blekhman, 2000]. The main operating modes of vibration setup are synchronization and multiple synchronization of rotors. The multiple synchronization mode is important from the point of view of ensuring stable vibration conveying regimes due to the creation of a non-zero average acceleration of the platform with a load. Ensuring a stable multiple synchronization mode at high rotation speeds is a challenging automation control problem [Zaitceva et al., 2023], [Andrievsky, Boikov, 2021].

One possible approach of vibration setup rotors synchronization control is the speed gradient algorithm, based on maintaining the required level of the total oscillation energy of the system [Andrievsky et al., 2021]. The energy-based approach has an advantage compared to algorithms based on feedback control of rotors speed. The movement of the load located on the platform significantly affects the system dynamics [Borisenok et al., 2024]. Therefore, it is advisable to use a comprehensive indicator of the vibrational state of the system, which in the speed gradient algorithm is the total oscillation energy of the system. The other related approaches to the problem can be found in [Zaitceva et al., 2025], [Tomchin et al., 2025].

The object of research is the processes of controlling the synchronization of rotation speeds of the rotors of the experimental mechatronic vibration setup SV-2M, which is a prototype of an industrial vibration setup. The speed gradient algorithm is used to rotors synchronization control.

The paper presents results of of experimental studies on the vibration setup. The influence of the completeness of information about the oscillatory energy of the system is demonstrated.

2 Experimental setup

The experimental two-rotor vibration setup SV-2M was developed at the Institute for Problems in Mechanical Engineering of the Russian Academy of Sciences for research and educational purposes and modified in 2025. The mechanical equipment of the complex is represented by a vibration stand, which operates using two unbalance vibration exciters. Each vibration actuator includes a three-phase asynchronous electric motor with adjustable rotational speed, a cardan shaft for transmitting rotational motion, and a vibration actuator in the form of an unbalanced rotor that rotates in a vertical plane on the stand's housing.

A lightweight, removable platform with containers of various capacities has been manufactured to accommodate the load. The platform base is made of 10 mm thick plywood. Holes are drilled in it for bolts that, using metal plates, fasten the base to the upper platform of the vibration setup. Additionally, holes are drilled in the plywood base for bolts securing the container. The bolt holes in the container bottoms are sealed to prevent spillage of the medium. The plywood base and the container are secured using wing nuts without the need for special tools. The mechanical part of the experimental mechatronic laboratory complex with the container installed is shown in Fig. 1.

Figure 1. Vibration setup SV-2M

3 Mathematical model

When developing the mathematical model of the vibration bench, the mathematical model proposed by O.P. Tomchina is taken as the basis [Tomchina, 2019]. The calculation scheme of the two-rotor vibration bench SV-2M with an attached load, moving in the vertical plane XY, is shown in Fig. 2. It is assumed that the displacements of the vibration installation in the direction Z are insignificant, meaning all motions occur in the plane OXY. The coordinates x_p and y_p describe the displacements of the platform in the moving coordinate system $O'X'Y'$. The coordinates x_g and y_g describe the displacements of the load. The quantity r determines the distance from the rotors to the axis X'. The platform is connected to the support frame by springs with stiffness c_x and c_y in the horizontal and vertical directions, respectively. The load is connected to the platform by springs with stiffness c_{gx} and c_{gy} in the horizontal and vertical directions, respectively. The coordinates of the spring attachment points are $\pm a$ in the horizontal direction. To obtain the differential equations, we use the

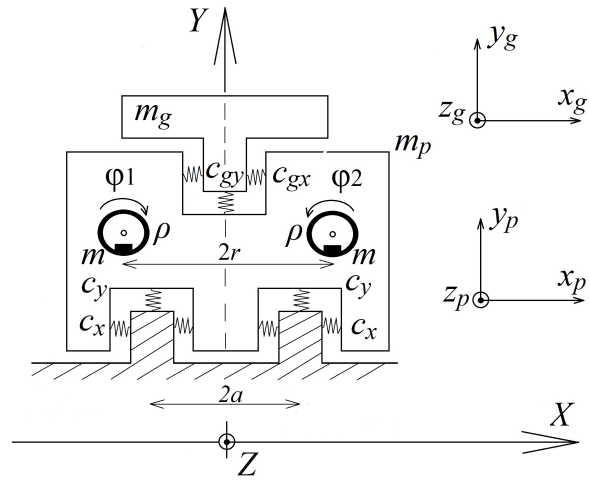

Figure 2. Kinematic scheme of the vibration setup

Lagrange equation of the second kind. Expressions for kinetic (T) and potential (Π) energy must be substituted into it. In the general case, these expressions will have the following form [Tomchina, 2022]:

$$
\begin{aligned}
T = {} & \frac{1}{2} m_p \left(\dot{x}_p^2 + \dot{y}_p^2\right) + \\
& + \frac{1}{2} \dot{\varphi}^2 \left(J + J_1 + J_2 - 2mr\rho \left(\cos\varphi_1 - \cos\varphi_2\right)\right) + \\
& + \frac{1}{2} \left(J_1 \dot{\varphi}_1^2 + J_2 \dot{\varphi}_2^2\right) - \\
& - m\rho \left(\sin\left(\varphi + \varphi_1\right) + \sin\left(\varphi + \varphi_2\right)\right) \dot{x}_p \dot{\varphi} + \\
& + m\rho \left(\cos\left(\varphi + \varphi_1\right) + \left(\varphi + \varphi_2\right)\right) y_p \dot{\varphi} + \\
& - m\rho \sin\left(\varphi + \varphi_1\right) \dot{x}_p \dot{\varphi}_1 + \\
& + m\rho \cos\left(\varphi + \varphi_1\right) \dot{y}_p \dot{\varphi}_1 - m\rho \sin\left(\varphi + \varphi_2\right) \dot{x}_p \dot{\varphi}_2 + \\
& + m\rho \cos\left(\varphi + \varphi_2\right) \dot{y}_p \dot{\varphi}_2 + \dot{\varphi}\dot{\varphi}_1 \left(J_1 - m\rho r \cos\varphi_1\right) + \\
& + \dot{\varphi}\dot{\varphi}_2 \left(J_2 - m\rho r \cos\varphi_2\right) + \frac{1}{2} m_g \left(\dot{x}_g^2 + \dot{y}_g^2\right),
\end{aligned}
$$

$$\Pi = (m_p + 2m)\, g y_p + \\ + m\rho g\left(\sin(\varphi+\varphi_1) + \sin(\varphi+\varphi_2)\right) + \\ + c_x\left(x_p^2 + a^2\cos^2\varphi\right) + c_y\left(y_p^2 + a^2\sin^2\varphi\right) + m_g g y_g \\ + \frac{1}{2}c_{gx}\left(x_p - x_g\right)^2 + \frac{1}{2}c_{gy}\left(y_p - y_g\right)^2.$$

In the work [Tomchina, 2023] it is shown that in this case the equations of dynamics of the vibration installation with the load will have the form:

$$\begin{aligned}
&m_p\ddot{x}_p - m\rho\sin(\varphi+\varphi_1)\ddot{\varphi}_1 - m\rho\sin(\varphi+\varphi_2)\ddot{\varphi}_2 \\
&- m\rho\left(\sin(\varphi+\varphi_1) + \sin(\varphi+\varphi_2)\right)\ddot{\varphi} - \\
&- m\rho\cos(\varphi+\varphi_1)\dot{\varphi}_1^2 - m\rho\cos(\varphi+\varphi_2)\dot{\varphi}_2^2 - \\
&- m\rho\left(\cos(\varphi+\varphi_1) + \cos(\varphi+\varphi_2)\right)\dot{\varphi}^2 - \\
&- 2m\rho\cos(\varphi+\varphi_1)\dot{\varphi}\dot{\varphi}_1 - 2m\rho\cos(\varphi+\varphi_2)\dot{\varphi}\dot{\varphi}_2 \\
&+ b\dot{x}_p + 2c_x x_p + c_{gx}\left(x_p - x_g\right) = 0, \\
&m_p\ddot{y}_p + m\rho\cos(\varphi+\varphi_1)\ddot{\varphi}_1 + m\rho\cos(\varphi+\varphi_2)\ddot{\varphi}_2 \\
&+ m\rho\left(\cos(\varphi+\varphi_1) + \cos(\varphi+\varphi_2)\right)\ddot{\varphi} - \\
&- m\rho\sin(\varphi+\varphi_1)\dot{\varphi}_1^2 - m\rho\sin(\varphi+\varphi_2)\dot{\varphi}_2^2 - \\
&- m\rho\left(\sin(\varphi+\varphi_1) + \sin(\varphi+\varphi_2)\right)\dot{\varphi}^2 \\
&- 2m\rho\sin(\varphi+\varphi_1)\dot{\varphi}\dot{\varphi}_1 - 2m\rho\sin(\varphi+\varphi_2)\dot{\varphi}\dot{\varphi}_2 \\
&+ m_p g + b\dot{y}_p + 2c_y y_p + c_{gy}\left(y_p - y_g\right) = 0, \\
&- m\rho\left(\sin(\varphi+\varphi_1) + \sin(\varphi+\varphi_2)\right)\ddot{x}_p \\
&+ \ m\rho\left(\cos(\varphi+\varphi_1) + \cos(\varphi+\varphi_2)\right)\ddot{y}_p \\
&+ \left(J + J_1 + J_2 - 2m\rho r\left(\cos\varphi_1 - \cos\varphi_2\right)\right)\ddot{\varphi} + \\
&+ \left(J_1 - mr\rho\cos\varphi_1\right)\ddot{\varphi}_1 + \left(J_2 + mr\rho\cos\varphi_2\right)\ddot{\varphi}_2 + \\
&+ 2m\rho r\sin\varphi_1\ \dot{\varphi}\dot{\varphi}_1 - 2m\rho r\sin\varphi_2\ \dot{\varphi}\dot{\varphi}_2 + \\
&+ m\rho r\sin\varphi_1\dot{\varphi}_1^2 - m\rho r\sin\varphi_2\dot{\varphi}_2^2 + \\
&+ m\rho g\left(\cos(\varphi+\varphi_1) + \cos(\varphi+\varphi_2)\right) \\
&+ c_\varphi\varphi + \ b_r\dot{\varphi} = 0, \\
&J_1\ddot{\varphi}_1 - m\rho\sin(\varphi+\varphi_1)\ddot{x}_p + m\rho\cos(\varphi+\varphi_1)\ddot{y}_p + \\
&+ \left(J_1 - m\rho r\cos\varphi_1\right)\ddot{\varphi} - \ m\rho r\cos\varphi_1\dot{\varphi}^2 + \\
&+ m\rho g\cos(\varphi+\varphi_1) + b_r\dot{\varphi}_1 = M_1, \\
&J_2\ddot{\varphi}_2 - m\rho\sin(\varphi+\varphi_2)\ddot{x}_p + m\rho\cos(\varphi+\varphi_2)\ddot{y}_p + \\
&+ \left(J_2 + m\rho r\cos\varphi_2\right)\ddot{\varphi} + \ m\rho r\sin\varphi_2\dot{\varphi}^2 + \\
&+ m\rho g\cos(\varphi+\varphi_2) + b_r\dot{\varphi}_2 = M_2, \\
&m_g\ddot{x}_g - c_{gx}\left(x_p - x_g\right) + b\dot{x}_g = 0, \\
&m_g\ddot{y}_g - c_{gy}\left(y_p - y_g\right) + b\dot{y}_g = -m_g g.
\end{aligned}$$

The following notations are introduced: φ_i is the rotation angle of the i-th rotor relative to the motor axis; M_i is the control torque on the i-th motor; b_r is the coefficient of viscous friction in the motor; b is the coefficient of viscous friction in the springs; m_p is the mass of the platform; ρ is the magnitude of the rotor eccentricity relative to the axis of rotation; J_i is the moment of inertia of the i-th rotor; m is the mass of the rotor imbalance; m_g is the mass of the load; g is the acceleration due to gravity. In the work [Tomchin et al., 2025] it is shown that taking into account the rotation of the platform has an extremely insignificant effect on the results of numerical simulation of the dynamics of this vibration bench. Therefore, setting $\varphi \to 0$, we obtain a system of equations of the form:

$$\begin{aligned}
&m_p\ddot{x}_p - m\rho\sin\varphi_1\ddot{\varphi}_1 - m\rho\sin\varphi_2\ddot{\varphi}_2 - m\rho\cos\varphi_1\dot{\varphi}_1^2 \\
&- m\rho\cos\varphi_2\dot{\varphi}_2^2 + b\dot{x}_p + 2c_x x_p + c_{gx}\left(x_p - x_g\right) = 0, \\
&m_p\ddot{y}_p + m\rho\cos\varphi_1\ddot{\varphi}_1 + m\rho\cos\varphi_2\ddot{\varphi}_2 - m\rho\sin\varphi_1\dot{\varphi}_1^2 \\
&- m\rho\sin\varphi_2\dot{\varphi}_2^2 + b\dot{y}_p + 2c_y y_p + c_{gy}\left(y_p - y_g\right) = -m_p g, \\
&J_1\ddot{\varphi}_1 - m\rho\sin\varphi_1\ddot{x}_p + m\rho\cos\varphi_1\ddot{y}_p + \\
&+ m\rho g\cos\varphi_1 + b_r\dot{\varphi}_1 = M_1, \\
&J_2\ddot{\varphi}_2 - m\rho\sin\varphi_2\ddot{x}_p + m\rho\cos\varphi_2\ddot{y}_p + \\
&+ m\rho g\cos\varphi_2 + b_r\dot{\varphi}_2 = M_2, \\
&m_g\ddot{x}_g - c_{gx}\left(x_p - x_g\right) + b\dot{x}_g = 0, \\
&m_g\ddot{y}_g - c_{gy}\left(y_p - y_g\right) + b\dot{y}_g = -m_g g.
\end{aligned}$$

4 Control System

The speed gradient algorithm is based on controlling the system based on the value of its total energy. The general form of the speed gradient algorithm can be written as [Andrievsky et al., 2021].

$$M = -\gamma\nabla_M\dot{Q}(z),$$

where M is the vector of control torques, $\dot{Q}(z)$ is the time derivative of the objective function $Q(z)$, ∇ is the gradient symbol, z is the vector of system state variables, γ is the tuning parameter of the control algorithm. To apply the speed gradient algorithm to the problems of controlling rotor synchronization, the objective function must include both a component that determines the output of the system's total energy to a specified level and a component that specifies the synchronization multiplicity. Such an objective function can be written as

$$Q(z) = 0.5\left((1-\alpha)\left(H - H^d\right)^2 + \alpha\left(\dot{\varphi}_1 \pm n\dot{\varphi}_2\right)^2\right),$$

where H^d is the setpoint for the value of the total oscillation energy of the system. Then the algorithm for controlling rotor synchronization based on the speed gradient will take the form

$$\begin{aligned}
M_1 &= -\gamma_1\left((1-\alpha)\left(H - H^d\right)\dot{\varphi}_1 + \alpha/J_1\left(\dot{\varphi}_1 \pm n\dot{\varphi}_2\right)\right), \\
M_2 &= -\gamma_2\left((1-\alpha)\left(H - H^d\right)\dot{\varphi}_2 \pm \alpha n/J_2\left(\dot{\varphi}_1 \pm n\dot{\varphi}_2\right)\right).
\end{aligned}$$

Here n is the synchronization multiplicity. The tuning parameters of the algorithm α, γ_1, γ_2 are selected experimentally. The plus or minus in the term defining the synchronization multiplicity is chosen depending on the direction of rotor rotation. This control algorithm was used in numerical simulation.

Within the development of control systems for the vibration unit, the task was to bring computer models of the vibration test bench as close as possible to the real setup. For experimental testing of control algorithms on the mechatronic test bench, it is necessary to convert the control torques into a signal supplied to the motor inputs. It is shown [Shagniev et al., 2023] that in steady-state operation, the electromechanical characteristic of an induction motor can be approximated by a linear combination of control and rotation speed . Typical mechanical characteristics of induction motors show a falling torque characteristic on the motor as the rotor speed increases. In general, the electromechanical characteristics of motors can be approximately described by the equations [Nguyen et al., 2025]

$$\tau_1 \dot{M}_1 + M_1 = k_1 u_1 - h_1 \dot{\varphi}_1,$$
$$\tau_1 \dot{M}_2 + M_2 = k_2 u_2 - h_2 \dot{\varphi}_2,$$

where u_1, u_2 are the dimensionless control signal at the motor inputs, M_1 and M_2 are the motor torque reduced to the gearbox output, τ_1 and τ_2 are the electromagnetic time constants of the motor. Obviously, the electromagnetic time constant, which for modern motors is on the order of milliseconds, is an order of magnitude lower than the oscillation periods of the structure at operating frequencies not exceeding 200 rad/s $\approx$ 32 Hz. Moreover, considering the presence of a frequency converter in the system, which itself essentially is an additional motor control system, it is advisable to assume that the values k_1, k_2, h_1, and h_2 are tuning parameters of the controller. The exact factory characteristics of the induction motors used in building the vibration test benches are unknown. Using the developments of the authors of [Blekhman et al., 2002], we choose the parameters determining the mechanical characteristics of the motors: $k_1 = k_2 = 0.00001$ Nm; $h_1 = h_2 = 0.01 \frac{\text{Nm·s}}{\text{rad}}$.

Let us write the expressions for the control moments as

$$M_1 = k_1 u_1 - h_1 \dot{\varphi}_1,$$
$$M_2 = k_2 u_2 - h_2 \dot{\varphi}_2.$$

Then the control signal takes the form

$$u_1 = \frac{M_1 + h_1 \dot{\varphi}_1}{k_1},$$
$$u_2 = \frac{M_2 + h_2 \dot{\varphi}_2}{k_2}.$$

where u_1, u_2 are the control inputs to the motors. It is assumed that the exact factory characteristics of the induction motors are unknown. Moreover, taking into account the presence of a frequency converter in the system, which itself essentially constitutes an additional motor control system, it is reasonable to consider the quantities k_1, k_2, h_1, and h_2 as adjustable parameters of the controller. Considering that in the actual setup the control input u is applied to the motor, we can obtain the final form of the control law:

$$u_1 = \frac{h_1 \dot{\varphi}_1}{k_1} - \frac{\gamma_1}{k_1}(1-\alpha)\left(H - H^d\right)\dot{\varphi}_1 - \\ - \frac{\alpha\gamma_1}{J_1 k_1}\left(\dot{\varphi}_1 \pm n\dot{\varphi}_2\right),$$
$$u_2 = \frac{h_2 \dot{\varphi}_2}{k_2} - \frac{\gamma_2}{k_2}(1-\alpha)\left(H - H^d\right)\dot{\varphi}_2 \pm \\ \pm \frac{\alpha n \gamma_2}{J_2 k_2}\left(\dot{\varphi}_1 \pm n\dot{\varphi}_2\right).$$

The structural diagram of the control system based on the speed gradient method is shown in Fig. 3. Thus, the

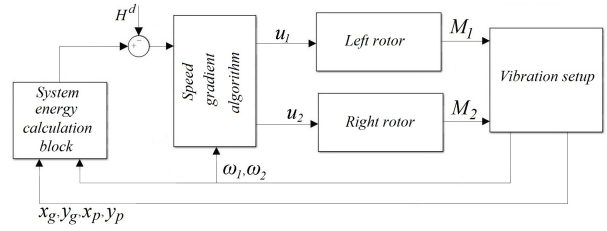

Figure 3. Structural diagram of the control system based on the speed gradient method

control law based on the speed gradient algorithm includes seven adjustable parameters, selected experimentally: α, γ_1, γ_2, k_1, k_2, h_1, and h_2. For simplification, algebraic transformations can be performed to reduce the number of these parameters, but this would lead to a loss of connection between the adjustable parameters that determine the electromechanical characteristics of the motors and their physical meaning, which would complicate the selection of values.

5 System Parameters and Partial Frequencies

For further total energy calculations, the following system parameters were chosen, consistent with the properties of the experimental vibration bench [Andrievsky, Boikov, 2021]:

$$m = 1.5\ kg;\ m_p = 32.1\ kg;\ m_g = 4.5\ kg;\ \rho = 0.04\ m;$$
$$g = 9.81\ kg \cdot m/s^2;\ J_1 = 0.0074\ kg \cdot m^2;$$
$$J_2 = 0.0074\ kg \cdot m^2; J = 0.2\ kg \cdot m^2;$$
$$b_r = 0.015\ N \cdot m \cdot s/rad; b = 5\ N \cdot s/m;\ r = 0.2\ m;$$
$$c_x = c_y = 8250\ N/m;\ c_{gx} = c_{gy} = 32250\ N/m.$$

Knowing the system parameters, its first partial frequencies can be estimated:

First partial frequency: $\omega_p \cong \sqrt{\frac{2c_y}{m_p + m_g}} \approx 21.2\ rad/s \approx 3.37\ Hz$;

Second partial frequency: $\omega_g \cong \sqrt{\frac{2c_{gy}}{m_g}} \approx 119.7\ rad/s \approx 19\ Hz$.

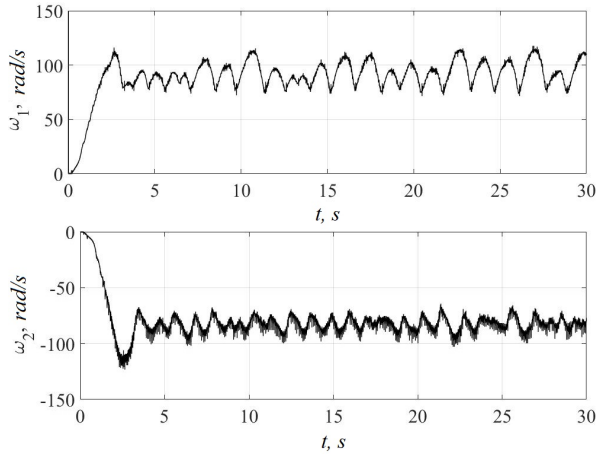

Figure 4. Processes of rotor angular velocities ω_1 and ω_2

6 Results

This section presents the results of experimental studies on the operation of the rotor synchronization control system based on the speed gradient method. The task for the control system is to reach the synchronization mode $H^d = 50\,\text{J}$, $n = 1$. Control algorithm parameters are $\gamma_1 = \gamma_2 = 0.1$, $\alpha_1 = \alpha_2 = 0.5$. It is assumed that there is no technical capability to estimate the displacements of the load. Let the measured total energy of the system include all terms from the expression.

$$\begin{aligned}\overline{H} = {} & 0.5m_p\left(\dot{x}_p^2 + \dot{y}_p^2\right) + 0.5J_1\dot{\varphi}_1^2 + 0.5J_2\dot{\varphi}_2^2 \\ & - m\rho\sin\varphi_1\dot{x}_p\dot{\varphi}_1 - m\rho\sin\varphi_2\dot{x}_p\dot{\varphi}_2 \\ & + m\rho\dot{y}_p\left(\cos\varphi_2\dot{\varphi}_2 + \cos\varphi_1\dot{\varphi}_1\right) + m_p g y_p \\ & + mg\rho\left(\sin\varphi_1 + \sin\varphi_2\right) + c_x x_p^2 + c_y y_p^2.\end{aligned}$$

The processes of rotor angular velocities $\omega_1 = \dot{\varphi}_1$ and $\omega_2 = \dot{\varphi}_2$ are shown in Fig. 4.

The processes of kinetic energy of rotor rotation $T_{rot} = \frac{1}{2}\left(J_1\dot{\varphi}_1^2 + J_2\dot{\varphi}_2^2\right)$, total system energy $H = T + \Pi$ and vertical platform velocity $\dot{y}_p$ are shown in Fig. 5.

Then the operation of the control system based on the speed gradient method with a reduced estimate of the system energy $\overline{H} = T_{rot} = \frac{1}{2}\left(J_1\dot{\varphi}_1^2 + J_2\dot{\varphi}_2^2\right)$ was considered . The same task for the control system is to reach the synchronization mode $H^d = 50\,\text{J}$, $n = 1$. The processes of rotor angular velocities $\omega_1 = \dot{\varphi}_1$ and $\omega_2 = \dot{\varphi}_2$ are shown in Fig. 6.

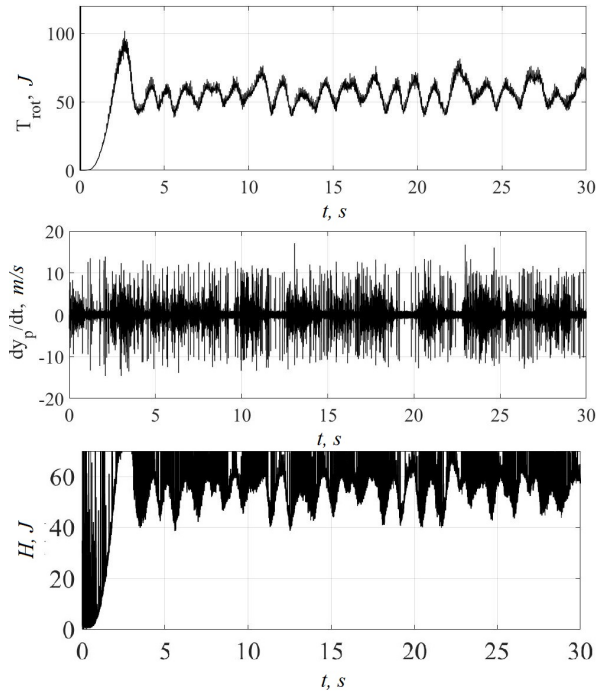

Figure 5. Processes of kinetic energy of rotor rotation T_{rot}, total system energy H and vertical platform velocity $\dot{y}_p$

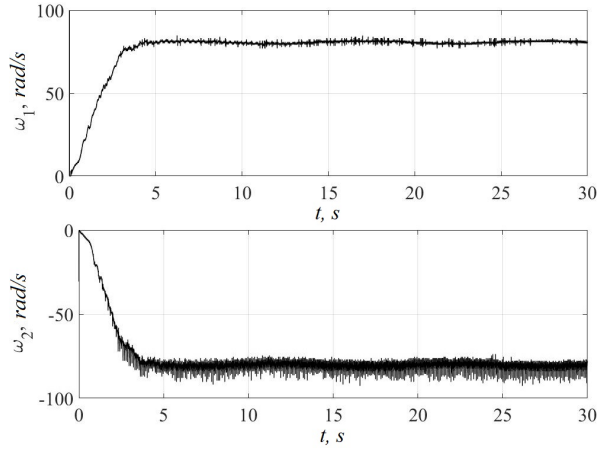

Figure 6. Processes of rotor angular velocities ω_1 and ω_2

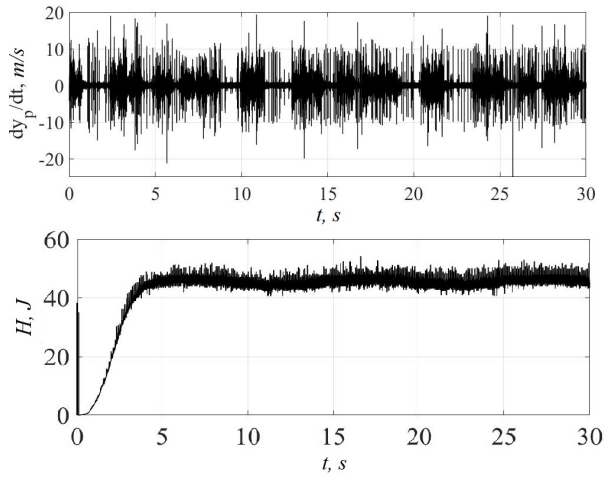

Figure 7. Processes of total system energy $H = T_{rot}$ and vertical platform velocity $\dot{y}_p$

The processes of total system energy H and vertical platform velocity $\dot{y}_p$ are shown in Fig. 7.

7 Conclusion

The obtained results substantiate the need to compensate for the incompleteness of information about payload dynamics by installing additional sensors or intellectualizing control systems [Gorbenko et al., 2025], [Shagniev, 2025], [Shagniev et al., 2023], [Shagniev, 2021].

Acknowledgements

The research was supported by the Ministry of Science and Higher Education of the Russian Federation (project no. 124041500008-1).

References

Andrievsky B.R., Fradkov A.L. Speed Gradient Method and Its Applications // Automation and Remote Control. – 2021. – Vol. 82, №. 9. – P. 1463 -1518.

Andrievsky B., Boikov V. Bidirectional controlled multiple synchronization of unbalanced rotors and its experimental evaluation // Cybernetics and Physics. – 2021. – Vol. 10, No. 2. – P. 63-74.

Blekhman I.I. Vibrational Mechanics. World Scientific: Singapore, 2000. – 536 p.

Blekhman I.I., Fradkov A.L., Tomchina O.P., Bogdanov D.E. Self-synchronization and controlled synchronization: General definition and example design // Mathematics and Computers in Simulation. – 2002. – Vol. 58, No. 4-6. – P. 367-384.

Borisenok S., Gogoleva E. Speed gradient control over qubit states // Cybernetics and Physics. - 2024. - Vol. 13, No. 3. – P.193-196.

Gorbenko I.D., Shagniev O.B. Intellectualization of the Drilling Process Control System with an Uncertain Workpiece Material // Mekhatronika, Avtomatizatsiya, Upravlenie. – 2025. – Vol. 26, № 3. – P. 119-127.

Nguyen B.H., Dang T.D., Furtat I., Gushchin P., Dao A.Q., Mai T.D. Control of direct current motors with guaranteed speed maintenance in given bounds // Cybernetics and Physics. – 2025. – Vol. 14, No. 2. – P. 148-153.v

Shagniev O.B., Fradkov A.L. Influence of Discretization on the Speed Gradient Synchronization Control // Mekhatronika, Avtomatizatsiya, Upravlenie. – 2023. – Vol. 24, №2. – P. 59-66.

Shagniev, O. B. Intellektualizatsiya sistemy upravleniya protsessom frezerovaniya v usloviyakh neopredelennosti // Avtomatizatsiya v promyshlennosti. – 2025. – No. 11. – P. 58-62. (In Russ.)

Shagniev O. Model Reference Neural Network Control for Two-rotor Vibration Unit // Proceedings of the V Scientific School "Dynamics of Complex Networks and their Applications" (DCNA 2021). – 2021. – p. 186-189.

Shagniev O.B., Tomchina O.P., Fradkov A.L. Learning Speed-Gradient Synchronization Control of the Two-Rotor Vibration Setup // IFAC-PapersOnLine. – 2022. – Vol. 55, No. 12. – P. 144-148.

Tomchin D., Gorlatov D. Control of a two-rotor vibration system with non-identical rotors and an elastically attached mass // Cybernetics and Physics. - 2025. - Vol. 14, No. 4. – P.??-??.

Tomchina O. P. Control of vibrational field in a vibration unit: influence of drive dynamics // Cybernetics and Physics. – 2019. – Vol. 8, No. 4. – P. 298-306.

Tomchina, O. P. Vibration field control of a two-rotor vibratory unit in the double synchronization mode // Cybernetics and Physics. – 2022. – Vol. 11, No. 4. – P. 245-251.

Tomchina O. Digital control of the synchronous modes of the two-rotor vibration set-up // Cybernetics and Physics. – 2023. – Vol. 12, No. 4. – P. 282-288.

Zaitceva Iu., Andrievsky B., Sivachenko L. Enhancing functionality of two-rotor vibration machine by automatic control // Cybernetics and Physics. – 2023. – Vol. 12, No. 4. – P. 289-295.

Zaitceva Iu., Bushuev D., Andrievsky B. Virtual testing of vibration mechatronic setup with technological accessories // Cybernetics and Physics. - 2025. - Vol. 14, No. 4. – P.??-??.